ORIGINAL ARTICLE

Dynamics of landscape patterns in an inland river delta of Central Asia based on a cellular automata-Markov model

Geping Luo · Tureniguli Amuti · Lei Zhu ·
Bulkajyr T. Mambetov · Bagila Maisupova ·
Chi Zhang

Abstract The analysis of landscape pattern changes is of significant importance for understanding spatial ecological dynamics and maintaining sustainable development, especially in wetland ecosystems, which are experiencing indirect human disturbances in arid Central Asia. This study attempted to examine the temporal and spatial dynamics of landscape patterns and to simulate their trends in the Ili River delta of Kazakhstan through quantitative analysis and a cellular automata (CA)-Markov model. This study also sought to examine the effectiveness of using the CA-Markov model for investigating the dynamics of the wetland landscape pattern. The total wetland area, including the river, lake, marsh, and floodplain areas, and the area of sandy land have remained steady, while that of desert grassland has decreased slightly, and shrublands have increased slightly from approximately 1978 to 2007. However, the wetland and shrubland areas exhibited a trend of increasing by 18.6 and 10.3 %, respectively, from 1990 to 2007, while the desert grassland and sandy land areas presented the opposite trend, decreasing by 30.3 and 24.3 %, respectively. The landscape patterns predicted for the year 2020 using probabilistic transfer matrixes for 1990–2007 (Scenario A) and 1990–1998 (Scenario B), respectively, indicated that the predicted landscape for 2020 tends to improve based on Scenario A, but tends to degrade based on Scenario B. However, the overall Kappa coefficient of 0.754 for the 2020 predicted landscapes based on Scenarios A and B indicates that the differences in the predicted landscapes are not distinct. This research indicates that the applied CA-Markov model is effective for the simulation and prediction of spatial patterns in natural or less disturbed landscapes and is valuable for developing land management strategies and reasonably exploiting the wetland resources of the Ili River delta.

Editor: Juan Ignacio Lopez Moreno.

G. Luo (✉) · T. Amuti · C. Zhang
State Key Laboratory of Desert and Oasis Ecology, Xinjiang Institute of Ecology and Geography, Chinese Academy of Sciences, Ürümqi 830011, Xinjiang, China
e-mail: luogp@ms.xjb.ac.cn

T. Amuti
e-mail: hturangul@gmail.com

C. Zhang
e-mail: zc@ms.xjb.ac.cn

T. Amuti
Graduate University of Chinese Academy of Sciences, Beijing 100049, China

L. Zhu
College of Prataculture and Environment Science, Xinjiang Agricultural University, Ürümqi 830052, Xinjiang, China
e-mail: smartzhulei04@163.com

B. T. Mambetov · B. Maisupova
Almaty Branch of Kazakh Scientific Research Institute of Forestry, Ministries of Agriculture, Almaty, Republic of Kazakhstan
e-mail: los-almaty@mail.ru

B. Maisupova
e-mail: Bagila.Maisupova@mail.ru

Introduction

The dynamics of landscape patterns are regarded as one of the most important sources of alterations in land surfaces, and they have a significant influence on the climate variability, biodiversity, water runoff and erosion, and soil degradation (Georgescu et al. 2009). Studies on landscape pattern dynamics generally focus on examining land use/land cover (LULC) changes and their driving forces (Loveland et al. 2002; Burgi et al. 2004) via modeling historical LULC changes and predicting future trends (Veldkamp and Lambin 2001; Verburg et al. 2004a, b; Hepinstall et al. 2008). Moreover, human-disturbed landscapes are often selected to analyze the dynamics of these patterns due to the difficulty of finding natural landscapes that have rarely been affected by human activities. However, determining the dynamics of natural landscape patterns is necessary for understanding human contributions to ecological processes through comparisons between natural and human-induced landscapes.

A number of simulation models have been developed for examining landscape dynamics (Verburg et al. 2004a, b), such as the conversion of land use and its effects (CLUE) (Verburg et al. 2002), cellular automaton (CA), Markov model, vegetation dynamic development tool/tool for exploratory landscape scenario analysis (VDDT/TELSA), simulating patterns and processes at landscape scales (SIMPPLLE), and rocky mountain landscape simulator (RMLANDS). However, each model has its own weaknesses and strengths, and no single approach is optimal and applicable to all cases (Verburg et al. 2008). To capture the scale, temporal, and spatial characteristics of landscape and explicitly address them, the integration of currently existing models of landscape dynamics could be a feasible solution (Luo et al. 2010). A Markov process is a discrete random process whose future probability depends only on its probability of the previous state. Although Markov models, as a type of stochastic model, provide a good analogy to natural landscape systems, they are not appropriate for strongly human-disturbed landscape, whose dynamics are not stochastic (Boerner et al. 1996; Weng 2002). However, a discrete-time Markovian model could lead to unreliable results and a misinterpretation of complex patterns because spatial relationships can strongly alter persistence and coexistence. As a result, it is necessary to incorporate a spatially explicit analysis of the interaction between neighboring landscape patterns to understand complex and dynamic landscape patterns (Verburg et al. 2004a, b). An explicitly spatial CA model has been developed to represent spatial and time-dependent processes and the nonlinear behavior of complex systems, such as forest dynamics or planning (Lett et al. 1999), urban growth, and land use change (Stevens and

Dragicevic 2007; Stevens et al. 2007). CA means that the model's decision concerning whether to change the state of a pixel explicitly takes the state of the neighboring pixels into consideration (Pontius and Malanson 2005). Therefore, an integrated model that is obtained by combining Markov chains and CA might represent an effective way to model the landscape dynamics (Caruso et al. 2005; Pontius and Malanson 2005; Guan et al. 2011) because the temporal and spatial dynamics of landscape patterns are controlled by the stochastic behaviors of the Markov chain process and the spatial dimension of the transition rules.

To identify the characteristics of natural landscape pattern dynamics, the Ili River delta in Central Asia was selected as the study area. The landscape pattern dynamics of this region correspond to natural landscape characteristics, which show random evolution and ecological stability overall, and their principal driving forces are physical environmental factors, such as the climate variability and runoff flow (Kipshakbaev and Abdrasilov 1994; Sivanpillai et al. 2006). Although the effects of human-induced disturbances (e.g., the construction of the Kapchagai reservoir and land reclamation in the upper or middle reaches of the river) are obvious in this area, the direct human disturbances have had relatively weak impacts on the Ili River delta between 1978 and 2007. Furthermore, the Ili River delta, which is one of the largest inland deltas in Central Asia, exhibits a high scientific and educational value, which is associated with increasingly widespread human disturbance (Kezer and Matsuyama 2006; Propastin 2008). Most studies that have been conducted in the region to date have focused on the investigation of the dynamic characteristics of the hydrology and climate of the Balkhash Lake basin (Mikhailov 2004; Lal et al. 2007; Hwang et al. 2011), but there is little information that is available about the dynamics of the landscape patterns in the area, mainly because there is limited accessible monitoring data and a lack of appropriate research methodologies.

The objectives of this study were (1) to analyze the landscape pattern changes and their possible driving forces in the Ili River delta during the period of from approximately 1978 to 2007, (2) to develop an integrated model that is based on a Markov model and a CA model and to validate that model using landscape type data that is derived from Landsat images that were obtained from approximately 1978 to 2007, and (3) to apply the developed model to predict future trends in landscape patterns for the next 20 years. This research will provide a fundamental resource for analyzing the underlying causes of landscape pattern changes, and its results have environmental and socioeconomic implications that are related to sustainable land use planning and decision-making.

Materials and methods

Study area

The Ili River delta in southeastern Kazakhstan (46°15′ N, 74°30 E′) (Fig. 1) is the largest wetland in the Lake Balkhash basin. The Ili River has a length of 1,439 km, 815 km of which lies within Kazakhstan. This river is formed by the confluence of the Kunges and Tekes Rivers flowing from the eastern Tianshan Mountains. The river flows west across the China–Kazakhstan border through the sandy Saryesik-Atyrau Desert and the Kapchagai reservoir, and finally, it flows into Lake Balkhash, forming the Ili River delta, which has vast wetland regions that consist of lakes, marshes, and jungle-like vegetation. The total area of the Ili River delta exceeds 10,000 km^2 (Propastin 2008), of which the wetland areas occupy over 4,000 km^2, accounting for approximately 37 % of the total area. The Kapchagai reservoir is located in the middle reaches of the Ili River and began to be filled in 1970. It exhibits an area of 1,850 km^2, with a water storage capacity of 28.1 km^3, and it is used for the production of electric energy and the long-term regulation of water flow. The climate of the Ili River delta is temperate continental, with distinct variations between seasons. The annual average temperature is approximately 5.6 °C, and the annual precipitation is approximately 150 mm (Sivan-pillai et al. 2006). The dominant vegetation in the study area consists of reeds, including *Calamagrostis pseudophragmites* and *Phragmites communis* in the floodplain areas.

Data collection and processes

Four types of data sets were used (see Table 1), including (1) Landsat MSS, TM, and ETM images that were used to map the land cover distribution; (2) land cover survey data that were collected in May 2009 and June 2012, and Google Earth^{TM} images that were used for selecting sampling plots for accuracy assessment; (3) hydrological data on the fluvial runoff volume of the Ili River over the past 40 years (1953–1992) and water levels of Lake Balkhash over the past 53 years (1953–2005) (Tacis Central Asia Action Programme 2006 2010a, b), which were used to account for the landscape dynamics; and (4) socioeconomic data that were obtained between 1970 and 2007, and ancillary topographic data that were used to develop criteria for making decisions for various land cover type transitions in the simulation of the CA-Markov approach.

Radiometric and atmospheric calibration was conducted for the Landsat images using the image-based dark-object subtraction method (Chander et al. 2009). The MSS images generally exhibit an original spatial resolution of

Fig. 1 Map showing the location of the study area
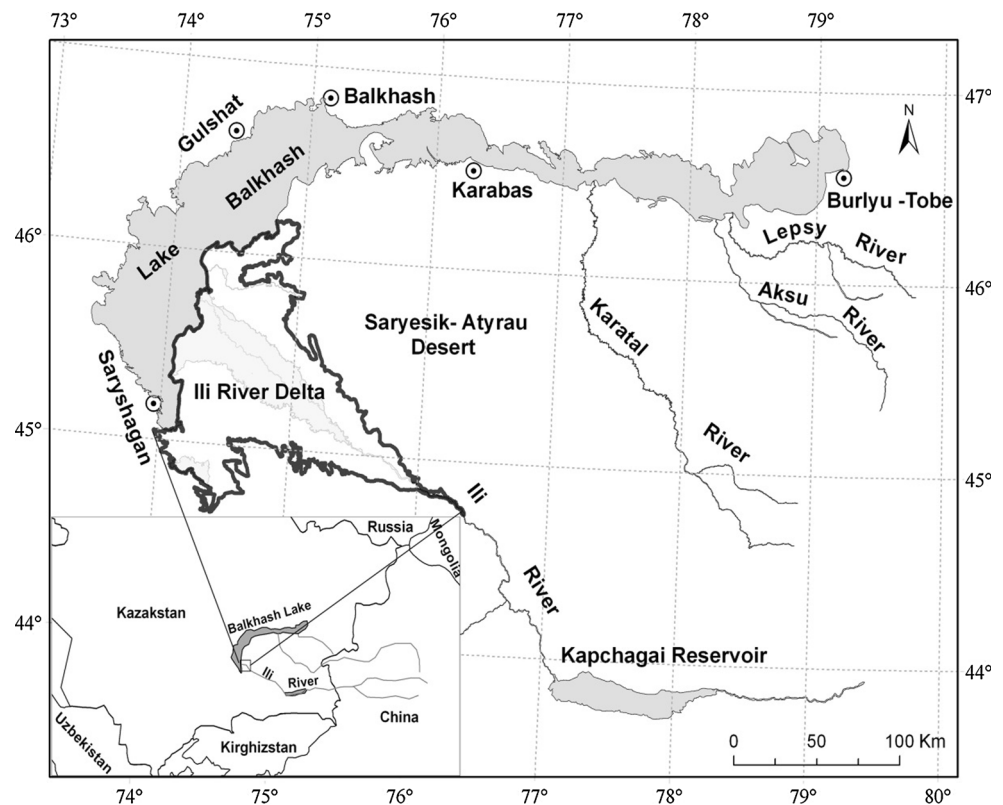
57 m × 79 m, whereas Landsat TM or ETM images show a spatial resolution of 30 m. All of the images were geometrically registered in the WGS_1984 UTM coordinate system (Zone 44, North) using Transverse_Mercator projection with a geometric error of less than one pixel, in such a way that all of the images exhibit the same coordinate system. The nearest-neighbor resampling technique was employed to resample the Landsat images to a pixel size of 30 m × 30 m during the image-to-image registration.

The land cover classification system that was used in this study consisted of wetland (e.g., rivers, lakes, marshes, floodplains), shrubland, desert grassland, and sandy land, according to the wetland classification system of China (Niu et al. 2009; Gong et al. 2010) and the international land cover classification system for arid landscapes (Anderson et al. 1976). Online Resource 1 describes the definitions of the land cover classes.

For historical remote sensing data, land use/land cover classification is often difficult due to the lack of sufficient training samples that can be used for image classification. A supervised classification algorithm based on a decision tree classifier coupled with principal component and textural analyses was employed for image classification in this study, which was useful for distinguishing different types of wetlands and other landscape types (Baker et al. 2006). Decision tree learning is a supervised classification method in which the learned function (based on the training data) is represented by a decision tree. This method is a hierarchal top-down approach that performs binary recursive partitioning on the basis of a set of tests that are defined at each branch (or node) in the tree to automatically allocate the

maximum information-carrying features for classification and discards the remaining features at that transitional stage. Thus, it is an efficient tool for land cover classification. This hierarchically based classification approach allowed us to avoid the dilemma of the lack of training samples that were available for historical remote sensing data and made full use of analysts' experiences and knowledge for accurately mapping the land cover distribution.

A post-classification comparison/refinement method that involves visual manual editing was applied to detect land use/land cover change trajectories. The errors that occurred at the class boundaries due to a spectral mixture within the pixels were replaced with values that were based on their surroundings using majority analysis. Any other spectrally confused pixels were re-coded into their correct land cover classes, while referring to visual interpretations. Finally, land cover maps were generated for four dates (Fig. 2): a circa 1978 land cover map based on Landsat MSS images from 22 August 1977 and 31 August 1979; and land cover maps for 1990, 1998, and 2007, which were based on TM images (25 May 1990, 2 May 1990; 28 September 1998, 3 September 1998), and ETM images (13 September 2007 and 19 September 2007).

An accuracy assessment of the classification results from the 2007 Landsat TM images was conducted using a total of 300 ground reference points from high-resolution images (1–5 m) of Google Earth and topographic maps. The Kappa coefficient can be used to analyze the accuracy assessment of the land cover classification by comparing the classification results with ground reference points from high-resolution images of Google Earth, and in addition, it can also be used to measure the similarity of two images, which can be applied to assess the stationarity of the landscape. The Kappa coefficient (KC) is calculated as

$$KC = (P_o - P_e)/(1 - P_e) \qquad (1)$$

where P_o is the percentage of the observed agreement, and P_e is the percentage of the expected agreement. The values of KC ≥ 0.75 were considered to have excellent agreement, 0.4–0.75 good agreement, and less than 0.4 poor agreement (Donker et al. 1993).

Model description

Although a Markov model can be used as a convenient tool for land cover modeling through a transition probability matrix over a specified time period, it provides no spatial information on the occurrence of land cover transformations. The integration of a Markov model with a dynamic spatial CA model, i.e., the CA-Markov model, can overcome the inherent limitations in each model and provides a means of simulating and predicting the temporal and

Table 1 Landsat images used in this research

Sensor data	Acquisition date; path/row; cloud cover (%)	Spectral and spatial resolutions
MSS	22 Aug. 1977; 162/29; 0 %	Four visible and near infrared bands with a 79-m spatial resolution
	31 Aug. 1979, 163/28; 0 %	
TM	26 May 1990; 150/29; 0 %	Three visible bands (blue, green, and red), one near infrared (NIR) band, and two shortwave infrared (SWIR) bands with a 30-m spatial resolution
	2 June 1990; 151/28; 0 %	
	28 Sept. 1998; 151/29; 1 %	
	3 Sept. 1998; 152/28; 0 %	
ETM	13 Sept. 2007; 151/29; 0 %	The same as TM, but including one panchromatic band with a 15-m spatial resolution
	19 Aug. 2007; 152/28; 0 %	

Fig. 2 Land cover changes for the Ili River delta during circa 1978–2007
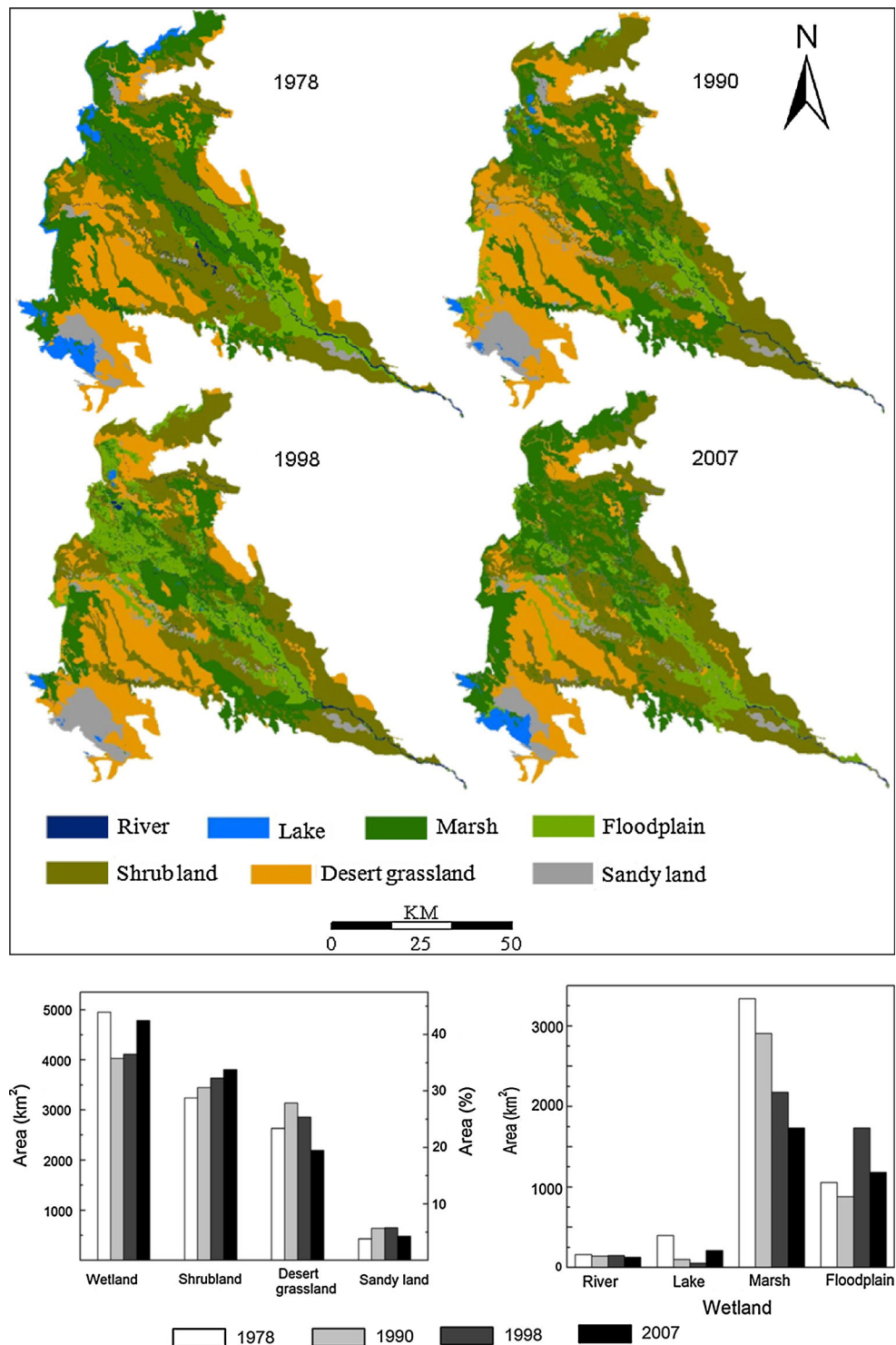
spatial dynamics of the landscape patterns (Shafizadeh and Helbich 2013; Mondal and Southworth 2010; Guan et al. 2011; Kamusoko et al. 2009).

The IDRISI program involves two techniques, i.e., Markov chain analysis and cellular automata (Eastman 1999). The task of the CA-Markov model was accomplished in the IDRISI software package. The main procedures for this operation in this study are given in Online Resource 2.

The CA-Markov model in the IDRISI program uses land cover maps, transition probability matrices produced via Markov analyses, and a collection of suitability maps to

output land cover projections (Schneider and Pontius 2001). This approach begins with an iterative process of reallocating the land cover until it meets the areal totals that are predicted by the Markov model, where the land cover changes develop as a growth process in the areas of high suitability that are proximate to existing areas according to transition rules, which are based on local spatiotemporal contiguity (Pontius and Malanson 2005).

It is essential to test whether the landscape pattern dynamics of the Ili River delta can be characterized by independence/randomness and stationarity/homogeneity. Only when it meets the assumptions of randomness and stationarity of landscape change, can a Markov model be used to describe or project the landscape processes. The Kappa coefficient of agreement can be used to test the stationarity of the landscape processes.

Pearson's chi-square (χ^2) test was also applied to test the independence of the landscape processes between successive time steps. Pearson's χ^2 is a distributed χ^2 that has $(n-1)^2$ degrees of freedom, where n indicates the number of land cover classes.

Results

Accuracy assessments of land cover classifications

The classification accuracies for the 2007 land cover classification are summarized in Online Resource 3. The 2007 Landsat ETM produced a high overall classification accuracy of 88.7 % and a Kappa coefficient of 0.845, which means that there was a good classification result (Donker et al. 1993).

Accuracy assessments were not conducted for other land cover classification results due to the lack of reference data. However, the accuracy of these results was believed to be similar to the accuracy of the 2007 land cover map, partly because of the applied hierarchically based classification approach. The stratification of land cover classes reduced the spectral confusion among the different land use/land cover classes; the analyst's knowledge and experience obtained from field surveys and Google Earth™ images were employed in merging the clusters into meaningful land cover classes, and manual editing in each step and post-processing further removed the misclassified classes that could not be automatically separated from the spectral signatures. One advantage of this method is that it does not require training samples during image classification, which is critical for the land use/land cover classification that is based on historical remote sensing data.

Based on the analysis described above, the results and accuracy of the classification from approximately 1978 to 2007 can be applied to the analysis of landscape pattern changes in this study.

Land cover changes from approximately 1978 to 2007

Wetlands, shrublands, and desert grasslands were found to be the dominant landscape types in the Ili River delta (Fig. 2; Table 2). The total wetland area, including river, lake, marsh, and floodplain, and sandy land area remained the same from approximately 1978 to 2007. However, in the areas that fall under wetland classification grade II, the lake, marsh, and floodplain areas initially experienced a decrease from approximately 1978 to 1990, and then, they gradually increased from approximately 1990 to 2007. The area of desert grassland expanded by 20 % from approximately 1978 to 1990 and then continually decreased, mainly being replaced with shrubland, marshes, and floodplains. The area of sandy land was expanded by 50.6 % from approximately 1978 to 1990 due to conversion from desert grassland and shrubland. After 1990, the area of sandy land decreased and gradually returned to the level that was observed from approximately 1978 to 2007. The area of shrubland continued to increase, mainly due to a transition from wetlands and desert grasslands. It was evident that the patterns of landscape change in the Ili River delta remained relatively stable from approximately 1978 to 2007, although periodic changes occurred in marsh, lake, floodplain, desert grassland, and sandy land areas. However, wetland and shrubland areas increased by 18.6 and 10.3 %, respectively, from 1990 to 2007, whereas desert grassland and sandy land areas presented the opposite trend, decreasing by 30.3 and 24.3 %, respectively.

The spatial distribution of the landscape in the Ili River delta presented vertical and horizontal characteristics due to the topographic and hydrological gradients in the area (Fig. 2). In general, wetlands tended to be situated next to the major river and were characterized by a vertical distribution along the major river course, giving priority to the marsh and floodplain areas on both sides of the river, whereas shrubland, desert grassland, and sandy land areas were distributed in the horizontal direction along the major river course. The desert grassland areas were aggregated in the southwestern delta, where the river network was sparse.

Testing and validation of the CA-Markov model

With a critical region of 0.05 for the chi-square test for the significance levels, the values of the test statistics were much larger than $\chi^2_{0.05}(7-1)^2 = \chi^2_{0.05}36 = 50.99$, which would indicate that the temporal landscape processes in the Ili River delta were independent from 1990 to 2007 (Iacono et al. 2012) (Table 3). Excluding the period of

Table 2 Observed areas of different landscape types in the Ili River delta in circa 1978, 1990, 1998, and 2007 and simulated areas for 2007 (km^2)

	Total area	Wetland					Shrubland	Desert grassland	Sandy land
		Area/%	River	Lake	Marsh	Floodplain	Area/%	Area/%	Area/%
Circa 1978 (observed)	11,257	4,956/44.0	161	398	3,340	1,057	3,240/28.8	2,629/23.4	431/3.8
1990 (observed)	11,257	4,030/35.8	143	101	2,905	881	3,448/30.6	3,142/27.9	637/5.7
1998 (observed)	11,257	4,114/36.5	150	53	2,176	1,734	3,632/32.3	2,861/25.4	649/5.8
2007 (observed)	11,257	4,781/42.5	129	212	3,258	1,182	3,804/33.8	2,190/19.5	482/4.3
2007 (simulated)	11,257	4,231/37.6	155	34	2,000	2,040	3,669/32.6	2,709/24.1	650/5.8
Kappa coefficient (2007)		0.895	0.878	0.101	0.324	0.635	0.658	0.838	0.862
RE (%) (2007)		11.50	16.93	517.96	62.87	42.11	3.66	19.18	25.89

RE relative error = (simulated − observed)/observed × 100 %

Table 3 Values of the χ^2 (significance level: 0.05) and Kappa coefficients in different periods

	1990–1998	1998–2007	1990–2007
χ^2	1.0×10^7	1.65×10^7	1.37×10^7
Kappa coefficients	0.815	0.788	0.762

approximately 1978–1990, the Kappa coefficients for the period from 1990 to 2007 were all greater than 0.75 (Table 3). This finding means that the landscape change in the Ili River delta could be described by a Markov process from 1990–2007.

Three data sets, i.e., the land cover base map for 1990, the transition suitability maps for 1998, and the 1990–1998 transition area matrix (see Online Resource 4), were integrated using a CA spatial filter to simulate the landscape pattern for 2007. Assuming 1998 as the initial time point of the prediction, a total of nine iterations were specified during the simulation because of the 9-year difference between 1998 and 2007. With each CA spatial low-pass filter, each land cover suitability map is re-weighted based on a 5 × 5 contiguity filter, which determines the location of the simulated landscape type (Pontius and Malanson 2005). Within each time step, the re-weighted suitability maps are run through a multi-objective land allocation (MOLA) process to spatially and explicitly allocate land cover classes. The MOLA process resolves land allocation conflicts by allocating the cell to the objective for which its weighted suitability is highest, thus reducing the size of the area to be assigned to each land cover class (Houet and Hubert-Moy 2006). The allocation considers land use suitability, the inherited attribute and the neighborhood effect using the CA model. How much land is allocated to a land cover type over the n-year period is determined by the transition area matrix derived from the Markov model

(Myint and Wang 2006). At the end of each step, a new simulated landscape map is generated by overlaying all of the results of the land allocation procedure.

The simulated map for 2007 was compared with the observed land cover map that was obtained from ETM images for 2007 (Table 2; Fig. 3). The overall Kappa coefficient between the simulated and observed landscape maps for 2007 was 0.765, which basically meets the model's simulation accuracy requirement. However, the Kappa indexes for the land cover classes were different from one another. The Kappa coefficients of the simulated versus the observed river, desert grassland, and sandy land areas were greater than 0.84. Conversely, the accuracies of the simulations for the lake and marsh areas were poor, showing values of 0.1008 and 0.324, respectively. Therefore, the CA-Markov model cannot generally predict the changes in the lakes and marshes, which slightly reduces the overall prediction accuracy for the landscape. The reason for this result is that the lake and marsh areas in the study area show significant temporal changes because of periodic fluctuations in the water levels of Lake Balkhash and the indirect effects of increasing intense human activities since the 1960s, especially after the Kapchagai reservoir was filled in 1970.

Based on the analysis described above, the landscape change in the Ili River delta could be described by a Markov process from 1990 to 2007, and the CA-Markov model can be used to project future landscape changes based on the landscape changes observed in the Ili River delta from 1990 to 2007.

Prediction of the landscape patterns for 2020

The transition probability matrices obtained for 1990–2007 (Scenario A) and 1990–1998 (Scenario B), respectively, were applied to the landscape prediction for 2020. The

Fig. 3 Simulated versus actual landscape pattern in 2007
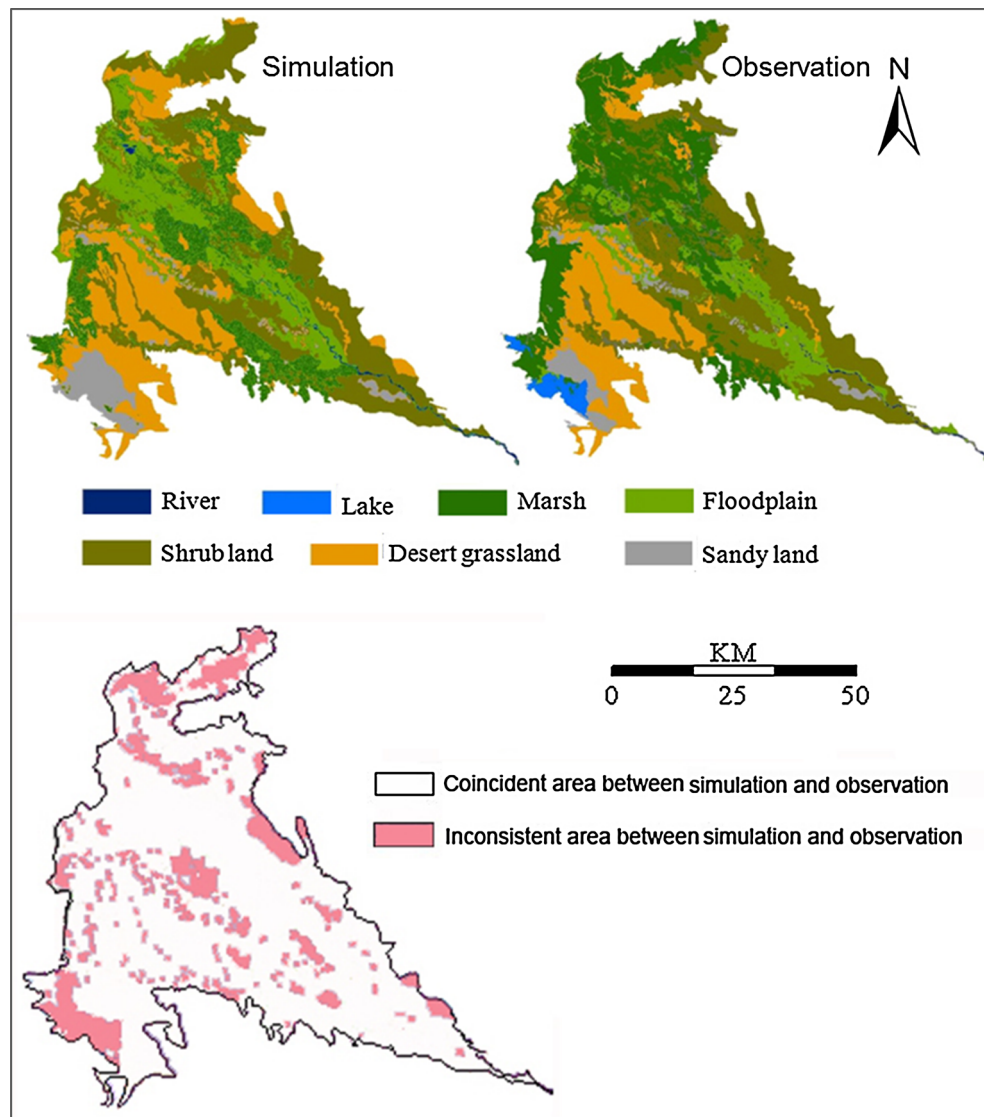
transition probability matrices for 1990–2007 and 1990–1998 are given in Online Resource 4. The landscape pattern maps predicted for 2020 were generated using the calibrated and validated CA-Markov model, assuming 1998 and 2007, respectively, as the initial time points of the prediction (Fig. 4; Table 4). Compared to the landscape pattern observed in 2007, for Scenario A, the wetland and shrubland areas were predicted to increase by 11.5 and 9.9 %, respectively, whereas those of desert grassland and sandy land would decrease by 33.0 and 38.4 %, respectively; for Scenario B, the wetland and shrubland areas were predicted to decrease by 7.3 and 3.4 %, respectively, whereas those of desert grassland and sandy land would increase by 14.6 and 32.5 %, respectively. The predicted landscape for 2020 tends to improve ecological conditions based on Scenario A but to generally degrade due to an

increase in desert grassland and sandy land based on Scenario B. However, the overall Kappa coefficient of 0.754 for the 2020 predicted landscapes based on scenarios A and B indicates that the predicted landscapes have excellent agreement (Donker et al. 1993). The wetlands do not experience large changes and generally stay steady in total amount in both scenarios, but several changes occur in the subclasses and the other main classes, and the differences and representation of the land cover classes also vary from one to another. The desert grasslands and sandy lands presented a high goodness-of-fit, with Kappa coefficients >0.75, while the lakes and marshes had the lowest degrees of agreement, with Kappa indexes that were under 0.30.

The spatial characteristics of the predicted landscape patterns for 2020 are similar to that of the landscape in 1998 and 2007. The landscape types that are related to

Fig. 4 Predicted distributions of land cover classes for 2020 with transitional probability matrices of 1990–2007 (Scenario A) and 1990–1998 (Scenario B), respectively, and their spatial differences
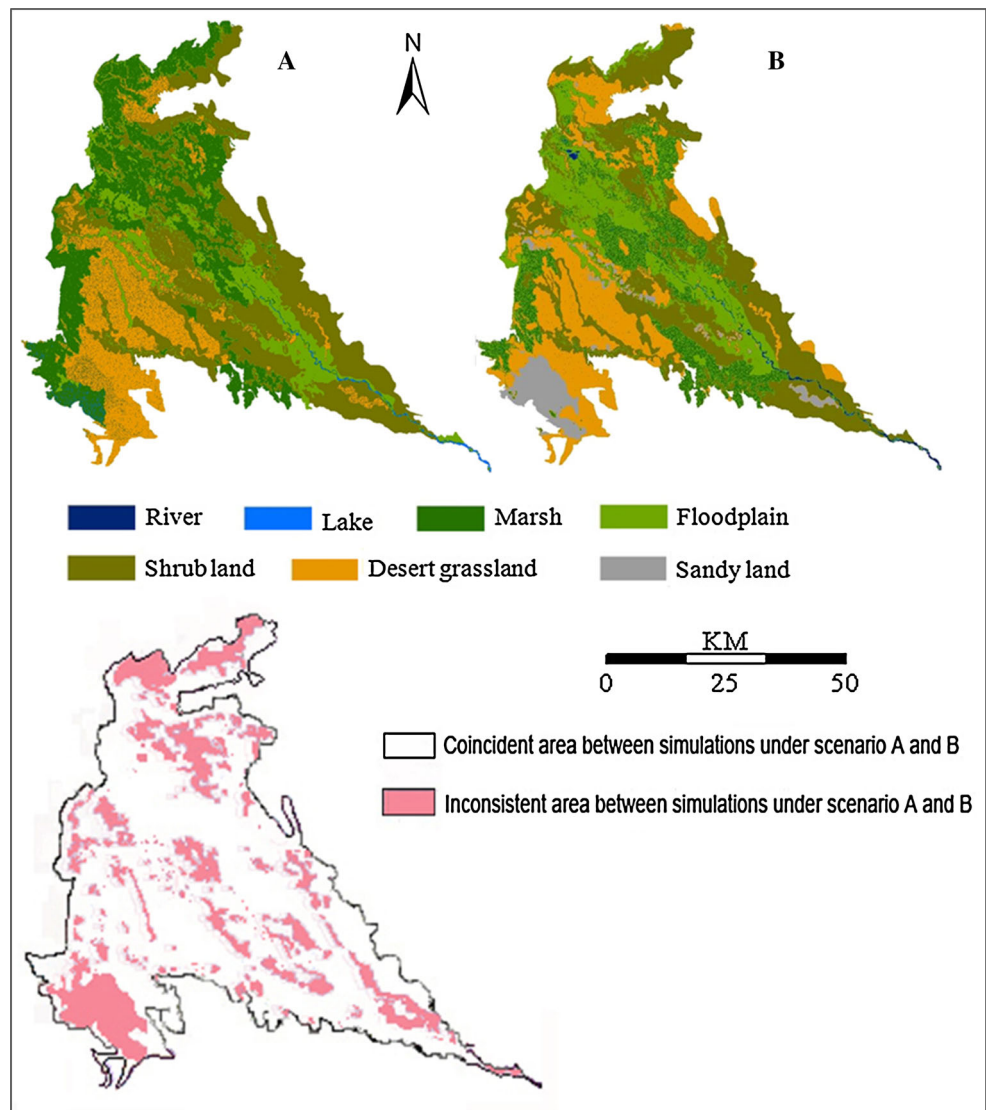

Table 4 Observed areas of different land cover classes in 2007 and projected areas for 2020 based on the transitional probability matrices for 1990–1998 and 1990–2007, respectively (km^2)

		Total area	Wetland					Shrubland	Desert grassland	Sandy land
			Area/%	River	Lake	Marsh	Floodplain	Area/%	Area/%	Area/%
Actual/2007		11,257	4,781/42.5	129	212	3,258	1,182	3,804/33.8	2,190/19.5	482/4.3
Projected/2020	Scenario A	11,257	5,312/47.6	101	289	3,891	1,031	4,180/37.1	1,468/13.0	297/2.6
	Scenario B	11,257	4,434/39.4	60	118	1,938	2,318	3,674/32.6	2,511/22.3	639/5.7
Change	Scenario A		531	−28	77	633	−151	376	−722	−185
	Scenario B		−347	−69	−94	−1,320	1,136	−130	321	157
Change (%)	Scenario A		11.5	−21.7	36.3	19.4	12.8	9.9	−33.0	−38.4
	Scenario B		−7.3	−53.5	−44.3	−40.5	96.1	−3.4	14.6	32.5

Scenario A: The projection situation for 2020 based on the transitional probability matrices for 1990–2007

Scenario B: The projection situation for 2020 based on the transitional probability matrices for 1990–1998

Change = projected − actual; Change (%) = (projected − actual)/actual × 100 %

wetlands are mainly distributed along the direction of the Ili River, giving priority to the marsh, floodplain, and shrubland on both sides of the river, the total area of which occupied 70.4–80.9 % of the entire delta. The desert grassland aggregated southwest of the sparse river network of the delta, where most of the marsh and desert grassland occurred. However, the distributions of the lake and sandy land have a degree of uncertainty. High potential transitions among the marshes, floodplains, and shrublands could result in more fragmentation of the landscape, weakening the landscape connectivity in the future. This circumstance will play an important role in the evolution of the landscape patterns of the Ili River delta.

Possible driving forces of the landscape dynamics

Regional climate variability and indirect human activities have contributed to altering the natural wetlands in the delta. The inflow of the Ili River to the delta is dependent on its upstream characteristics. Upstream, the annual precipitation of 386.8 and 406.5 mm during 1987–2009 and 1997–2007, increased by 10.1 and 15.7 %, respectively, compared with that of 351.4 mm during 1957–1986 (Sun et al. 2010; Abulaiti 2012). An average annual runoff yield of 15.9 km^3 upstream constitutes 69.5 % of the entire runoff of the Ili River (Wang and Lu 2009). The intense development of agricultural activities along the Ili River and Karatol River accelerated the water loss from Lake Balkhash from 1960 to 1985. The volume of the inflow of the Ili River to Lake Balkhash was 15 km^3 in 1970, which was sharply reduced to 7 km^3 in 1983 due to the construction of the Kapchagai hydroelectric power station in the 1970s (Hwang et al. 2011). The primary reason for the decrease in the area of the wetlands was the decline of the water level in the lake from 1970 to 1985, which is caused by a decrease in the inflow to Lake Balkhash. Figure 5 was created by integrating the scattered public references, including the upstream inflow, the inflow to Lake Balkhash, the water usage of the Ili River delta, the irrigation abstraction, and the water level of Balkhash (Wang and LU 2009; Tacis Central Asia Action Programme 2006 2010a, b; Xie et al. 2011; Abulaiti 2012). The upstream inflow of the Ili River was relatively stable, whereas the inflow to the lake was reduced significantly following the initiation of the filling of the Kapchagai reservoir in 1970 for agricultural irrigation and the production of electric energy. This change led to a continuous increase in water extraction for irrigation from the Ili River until 1991. The construction of the Kapchagai reservoir led to some additional adverse effects on the wetland ecosystems, such as altering the natural hydrological patterns, decreasing the size of the wetland areas, and decreasing the biodiversity (Tacis Central Asia Action
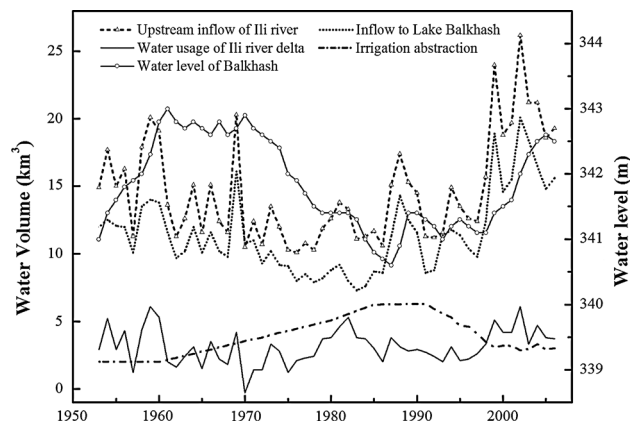

Fig. 5 Hydrological changes in the Ili River delta (derived from the scattered references related to lake Balkhash)

Programme 2006 2010a). However, following the collapse of the former Soviet Union in the early 1990s, the irrigated area of the Ili River basin significantly decreased, by 30 %, and the volume of water used for irrigation decreased by up to 53 % from 1990 to 2006 (Tacis Central Asia Action Programme 2006 2010a). The Kapchagay Dam was completed in late 1969 and began slowly filling the reservoir in 1970. Over a period of 16 years between 1970 and 1985, the volume of Lake Balkash declined by 39 km^3 to directly feed the Kapchagay Reservoir, and by 1987, Lake Balkash had reached the lowest lake level ever recorded. However, in 1988, this situation improved when the volume of Balkash increased once more from the river discharge from the east. In addition, the climate conditions favored an increased river runoff upstream of the Ili River watershed from 1986 to 2007 (Sun et al. 2010; Abulaiti 2012). These factors significantly increased the inflow to Lake Balkhash, contributing to the rise in the lake water level from 1990 to 2007 and a corresponding increase in the wetland areas in the Ili River delta.

However, regulation of the runoff of the Ili River has primarily altered the hydrological regime of the streams in the delta since the early 1990s, which would be highly advantageous for improving the maintenance of the vegetation system of Lake Balkhash and for the rehabilitation of wetland ecosystems in the Ili River delta (Abdrasilov and Tulebaeva 1994). The wetland landscape pattern of the Ili River delta presented significant fluctuations due to hydrological variability and indirect human disturbances.

Figure 5 shows that the changes in the lake water level and wetland landscape patterns in the Ili River delta have responded to climate-driven hydrological processes and human disturbances in the Ili-Balkhash basin. However, these changes were inconsistent, with the former lagging

behind the latter. For example, despite the relatively high water flow of the Ili River from 1988 to 1990 and the sharp reduction in the area of the irrigated lands in the Kazakhstan portion of the basin in the 1990s, desertification has become apparent along the Ili River as well as in the easternmost portion of the delta (Starodubtsev and Truskavetskiy 2011).

Discussion

Although the CA-Markov model is effective in simulating the overall dynamics of the natural landscape of the Ili River delta, it cannot precisely simulate the change in the landscape due to human disturbances, and certain errors and uncertainties exist in the results of the simulation. Some of these errors are mainly explained by the limitations of the image classification procedure and the inherent uncertainties in the model that result from the transition rules; some result from the neighborhood configuration, the time step, stochastic variables of the CA-Markov model, and the uncertainty in the natural factors coupled with human disturbances, such as fluctuations in the water inflow of the Ili River, which are primarily driven by climate variability.

Sensor noise, atmospheric disturbances, and limitations of the classification algorithms are possible sources of classification errors (Lu and Weng 2007). For example, some of the pixels could be misclassified with respect to their land cover types by employing classification techniques on remote sensing data. The existence of mixed pixels in remote sensing images also causes uncertainty for remote sensing classifications due to spatial resolution limitations. The land cover types that share similar spectral response patterns in the images make it difficult to identify pure patches and result in confusion in classification, especially in the nonvegetated area. Nevertheless, these result in uncertainties in the data sources for the simulation. In addition to data source errors, common GIS operations or transformations (e.g., vector–raster transformations or raster–raster transformations) can also bring about uncertainties in the CA modeling due to a loss in the spatial detail.

One of the inherent model uncertainties is the errors in the estimations of the parameters and calculating the transition rules using a predefined parameter matrix. In this study, two scenarios were designed to predict future landscape patterns with a validated CA-Markov model. There are some differences in the landscape patterns for 2020 because two different transition probability matrices were applied to landscape predictions during the simulation of the model. On the one hand, this approach can explain, to some extent, the inherent uncertainties in the model that result from the transition rules, and on the other hand, the degree of uncertainty in the model is also partly specified. The CA-Markov model considers a probability matrix of plausible future states with respect to a general trend for each landscape type and does not consider fluctuating changes that are derived from having a succession of landscape types driven by climate change (White and Engelen 2000; Yeh and Li 2003).

The neighborhood configuration is another problem in implementing the transition rules into computational models using discrete cells, which are only approximations to continuous space and have a loss of spatial detail; thus, how to choose the proper cell size and cell shape within a neighborhood can affect the outcome of the simulation. It is important to account for the influence of the total number of iterations (time steps) on the location of the simulated landscape types when the contiguity rule is applied because the definition of the edges is updated at each iteration of the time step. A small number of time steps will not allow spatial details to emerge during the simulation process, while a larger number of time steps can lead to more iterations and generate more accurate simulation results (Yeh and Li 2006).

Therefore, it is difficult to accurately predict the trends in some classes, such as lakes, marshes along the shoreline, and floodplains, which have shown nonstationarity to some extent. This finding suggests that the model's simulation accuracy increases with the stationarity of the natural landscape.

Conclusions

Using Landsat image-derived land cover data (obtained circa 1978, 1990, 1998 and 2007), our proposed combination model linked Markov chain analysis with a cellular automata model and was applied to simulate landscape pattern changes in the Ili River delta. This model was demonstrated to be an effective tool for conducting detailed research on a wetland landscape that is characterized by indirect human disturbances. The evolution of the landscape pattern from approximately 1978 to 2007 and the prediction for 2020 revealed that there is a different trend of landscape changes in the Ili River delta. The patterns of landscape change in the Ili River delta remained relatively stable from 1990 to 2007, although periodic changes occurred in marsh, lake, floodplain, desert grassland, and sandy land areas. However, wetland and shrubland areas showed an increasing trend from 1990 to 2007, whereas desert grassland and sandy land areas presented the opposite, decreasing trend. These observations could be closely related to the impacts of natural factors, such as climate-driven hydrological processes. The 2020 predicted

landscapes that are based on both scenarios indicate that the predicted landscapes have excellent agreement. The wetlands do not experience large changes and usually remain steady with respect to the total amount in both scenarios, but several changes occur to subclasses and other main classes. The errors in the land cover classification and the inherent uncertainties in the model might contribute to the uncertainty of the simulation and the projection that is based on the CA-Markov model.

Due to the inherent characteristics of the lake and river, the changes in lake water levels and wetland landscape patterns detected in the Ili River delta were inconsistent, and the former generally lagged behind the latter. This situation will result in some projection errors for the CA-Markov model.

As the CA-Markov model has been demonstrated to be useful for investigating certain types of landscapes with different landscape structures, CA-Markov projections for such landscapes can serve as an early warning system for the future effects of potential landscape changes. Land managers and decision makers could therefore evaluate the ecological and economic impacts of predicted landscape changes more effectively and implement alternative land use policies and conservation strategies as necessary.

References

Abdrasilov SA, Tulebaeva KA (1994) Dynamics of the Ili delta with consideration of fluctuations of the level Lake Balkhash. Hydrotech Constr 28:421–426

Abulaiti R (2012) Trends of precipitation over the Ili valley. Gansu Water Resour Hydropower Technol 48(7):1–4 (in Chinese)

Anderson JR, Hardy EE, Roach JT, Witmer RE (1976) A land use and land cover classification system for use with remote sensor data. US Geol Surv Prof Pap 964:1–36

Baker C, Lawrence R, Montague C, Patten D (2006) Mapping wetlands and riparian areas using Landsat ETM + imagery and decision-tree-based models. Wetlands 26:465–474

Boerner REJ, DeMers MN, Simpson JW, Artigas FJ, Silva A, Berns LA (1996) Markov models of inertia and dynamic on two contiguous Ohio landscapes. Geogr Anal 28:56–66

Burgi M, Hersperger AM, Schneeberger N (2004) Driving forces of landscape change—current and new directions. Landsc Ecol 19:857–868

Caruso G, Rounsevell M, Cojocaru G (2005) Exploring a spatio-dynamic neighbourhood-based model of residential behaviour in the Brussels periurban area. Int J Geogr Inf Sci 19:103–123

Chander G, Markham BL, Helder DL (2009) Summary of current radiometric calibration coefficients for Landsat MSS, TM, ETM + , and EO-1 ALI sensors. Remote Sens Environ 113:893–903

Donker DK, Hasman A, Van Geijn HP (1993) Interpretation of low kappa values. Int J Biomed Comput 33:55–64

Eastman JR (1999) Idrisi 32: user's guide. Clark University, Worcester

Georgescu M, Miguez-Macho G, Steyaert LT, Weaver CP (2009) Climatic effects of 30 years of landscape change over the Greater Phoenix, Arizona, region: 1. Surface energy budget changes. J Geophys Res Atmos 114:1–17

Gong P, Niu Z, Cheng X, Zhao K, Zhou D, Guo J, Liang L, Wang X, Li D, Huang H, Wang Y, Wang K, Li W, Wang X, Ying Q, Yang Z, Ye Y, Li Z, Zhuang D, Chi Y, Zhou H, Yan J (2010) China's wetland change (1990–2000) determined by remote sensing. Sci China Earth Sci 53:1036–1042

Guan D, Li H, Inohae T, Su W, Nagaie T, Hokao K (2011) Modeling urban land use change by the integration of cellular automaton and Markov model. Ecol Model 222(20–22):3761–3772

Hepinstall JA, Alberti M, Marzluff JM (2008) Predicting land cover change and avian community responses in rapidly urbanizing environments. Lands Ecol 23:1257–1276

Houet T, Hubert-Moy L (2006) Modelling and projecting land-use and land-cover changes with a cellular automaton in considering landscape trajectories: an improvement for simulation of plausible future states. EARSeL eProc 5:63–76

Hwang C, Kao Y-C, Tangdamrongsub N (2011) Preliminary analysis of lake level and water storage changes over lakes Baikal and Balkhash from satellite altimetry and gravimetry. Terr Atmos Ocean Sci 22:97–108

Iacono M, Levinson D, El-Geneidy A, Wasfi R (2012) A Markov chain model of land use change in the twin cities, 1958–2005. http://nexus.umn.edu/Papers/MarkovLU

Kamusoko C, Aniya M, Adi B, Manjoro M (2009) Rural sustainability under threat in Zimbabwe-Simulation of future land use/cover changes in the Bindura district based on the Markov-cellular automata model[J]. Appl Geogr 29(3):435–447

Kezer K, Matsuyama H (2006) Decrease of river runoff in the Lake Balkhash basin in Central Asia. Hydrol Process 20:1407–1423

Kipshakbaev NK, Abdrasilov SA (1994) Effect of economic activity on the hydrologic regime and dynamics of the Ili delta. Hydrotech Constr 28:416–418

Lal R, Suleimenov M, Stewart BA, Hansen DO, Doraiswamy P (2007) Climate change and terrestrial carbon sequestration in Central Asia. Taylor & Francis, London

Loveland TR, Sohl TL, Stehman SV, Gallant AL, Sayler KL, Napton DE (2002) A strategy for estimating the rates of recent United States land-cover changes. Photogramm Eng Remote Sens 68:1091–1099

Lu D, Weng Q (2007) A survey of image classification methods and techniques for improving classification performance. Int J Remote Sens 28:823–870

Luo GP, Yin CY, Chen X, Xu WQ, Lu L (2010) Combining system dynamic model and CLUE-S model to improve land use scenario analyses at regional scale: a case study of Sangong watershed in Xinjiang, China. Ecol Complex 7:198–207

Mikhailov VN (2004) The impact of deltas on the mean long-term water river runoff. Water Resour 31:351–356

Mondal P, Southworth J (2010) Evaluation of conservation interventions using a cellular automata-Markov model. For Ecol Manag 260(10):1716–1725

Myint SW, Wang L (2006) Multicriteria decision approach for land use land cover change using Markov chain analysis and a cellular automata approach. Can J Remote Sens 32:390–404

Niu Z, Gong P, Cheng X, Guo J, Wang L, Huang H, Shen S, Wu Y, Wang X, Wang X, Ying Q, Liang L, Zhang L, Wang L, Yao Q, Yang Z, Guo Z, Dai Y (2009) Geographical characteristics of China's wetlands derived from remotely sensed data. Sci China, Ser D Earth Sci 52:723–738

Pontius GR, Malanson J (2005) Comparison of the structure and accuracy of two land change models. Int J Geogr Inf Sci 19:243–265

Propastin PA (2008) Simple model for monitoring Balkhash Lake water levels and Ili River discharges: application of remote sensing. Lakes Reserv Res Manag 13:77–81

Schneider LC, Pontius RG (2001) Modeling land-use change in the Ipswich watershed, Massachusetts, USA. Agric Ecosyst Environ 85:83–94

Shafizadeh MH, Helbich M (2013) Spatiotemporal urbanization processes in the megacity of Mumbai, India: a Markov chains-cellular automata urban growth model. Appl Geogr 40:140–149

Sivanpillai R, Latchininsk AV, Driese KL, Kambulin VE (2006) Mapping locust habitats in River Ili Delta, Kazakhstan, using Landsat imagery. Agric Ecosyst Environ 117:128–134

Starodubtsev VM, Truskavetskiy SR (2011) Desertification processes in the Ili River delta under anthropogenic pressure. Water Resour 38:253–256

Stevens D, Dragicevic S (2007) A GIS-based irregular cellular automata model of land-use change. Environ Plan B Plan Design 34:708–724

Stevens D, Dragicevic S, Rothley K (2007) iCity: a GIS-CA modelling tool for urban planning and decision making. Environ Model Softw 22:761–773

Sun H, Chen Y, Li W, Li F, Chen Y, Hao X, Yang Y (2010) Variation and abrupt change of climate in Ili River Basin, Xinjiang. J Geogr Sci 20:652–666

Tacis Central Asia Action Programme 2006 (2010a) Development and improvement of policy instruments for environmental protection, Republic of Kazakhstan, EuropeAid/127636/C/SER/KZ, Ili-Balkhash LEAP: Task 3 report—hydrology, pp 1–34

Tacis Central Asia Action Programme 2006 (2010b) Development and improvement of policy instruments for environmental protection, Republic of Kazakhstan, EuropeAid/127636/C/SER/KZ, Result 3–1: Ili-Balkhash LEAP, pp 1–56

Veldkamp A, Lambin EF (2001) Predicting land-use change. Agric Ecosyst Environ 85:1–6

Verburg PH, Soepboer W, Limpiada R, Espaldon MVO, Sharifa M, Veldkamp A (2002) Land use change modelling at the regional scale: the CLUE-S model. Environ Manag 30:391–405

Verburg PH, de Nijs TCM, van Eck JR, Visser H, de Jong K (2004a) A method to analyse neighbourhood characteristics of land use patterns. Comput Environ Urban Syst 28:667–690

Verburg PH, Schot P, Dijst M, Veldkamp A (2004b) Land use change modelling: current practice and research priorities. GeoJournal 61:309–324

Verburg PH, Eickhout B, van Meijl H (2008) A multi-scale, multi-model approach for analyzing the future dynamics of European land use. Ann Reg Sci 42:57–77

Wang JY, Lu JX (2009) Hydrological and ecological impacts of water resources development in the Ili River Basin. J Nat Resour 24(7):1299–1310 (in Chinese)

Weng QH (2002) Land use change analysis in the Zhujiang Delta of China using satellite remote sensing, GIS and stochastic modelling. J Environ Manag 64:273–284

White R, Engelen G (2000) High-resolution integrated modelling of the spatial dynamics of urban and regional systems. Comput Environ Urban Syst 24:383–400

Xie L, Long A, Mi D, Wang J (2011) Study on ecological water consumption in delta downstream of Ili River. J Glaciol Geocryol 33(6):1330–1340

Yeh AGO, Li X (2003) Simulation of development alternatives using neural networks, cellular automata, and GIS for urban planning. Photogramm Eng Remote Sens 69:1043–1052

Yeh AGO, Li X (2006) Errors and uncertainties in urban cellular automata. Comput Environ Urban Syst 30:10–28